Journal of Ceramic Processing Research. Vol. 17, No. 9, pp. 956~960 (2016)

J O U R N A L O F
Ceramic Processing Research

Synthesis and photoluminesence properties of $NaCa_4(BO_3)_3$:xEu^{2+}, xCe^{3+} Co-doped with lanthanide

S. Isik[a,*], Y.Z. Halefoglu[b] and O. Serindag[c]

[a,c]*Department of Chemistry, Science and Arts Faculty, Cukurova University, 01330- Balcali /Adana, Turkey*

[b]*Department of Ceramic, Faculty of Art, Cukurova University, 01330- Balcali/Adana, Turkey*

A new borate compound $NaCa_4(BO_3)_3$:xEu^{2+},xCe^{3+} co-doped with Eu^{2+} and, Ce^{3+} was prepared by combustion synthesis method using rare-earth nitrates, urea, and boric acid as starting materials. The prepared sample was characterized through X-ray diffraction (XRD), scanning electron microscope (SEM), and fourier transform infrared spectra (FTIR). The energy dispersive x-ray spectrometer (EDX) confirmed the presence of the Na, Ca, B, O, Eu, and Ce. The photoluminescence (PL) excitation and emission spectra of the Eu^{2+}, Ce^{3+}co-doped $NaCa_4(BO_3)_3$were also investigated using spectrometer at room temperature.The excitation spectrum consists of an intense band peaking at 352 nm. The emission spectrum shows a single intensive band centered at 445 nm, which correspond to the $4f^65d^1$ -$4f^7$. For the excitation wavelength of 352 nm the emission intensity increases intially with the increase of lanthanide concentration and reaches to the maximum at x = 0.05 nm.The critical distance of concentration quenching, the luminescence lifetime have also been investigated.

Key words: Borates, Combustion method, Rare-earth, Pnosphors, Luminescence.

Introduction

The photoluminaescence properties (PL) of rare earth ions in borates have been studied extensively due to their application in the fields of fluorescent lamps, detector systems [1-4] and, whitelight emitting diodes (white LEDs) [5-7].

PL properties of cerium and europium ionshave been studied widely because of their application in the fields of lamps and display devices [8-10]. The emission of Ce^{3+} consist of a broad band with two peaks, which is due to the transition from 5d to the ground state. The d-f transition is an allowed electric dipole transition and therefore the decay time of fluorescence is short ($< 10^{-7}$s) enough to be applied in the field of lamps and display. The emission of Eu^{3+} ion in 4f shell is sensitive to the influence of the surroundings owing to the shielding effect 5s and 5p electrons, the luminescence properties of Eu^{+3} ions are strongly related to their chemical and structural environment inside the matrix [11, 12].

Among the most investigated matrices for rare earth activated phosphors, i.e., oxides, silicates, phosphates, aluminates, and borates are good candidates because of their low synthesis temperature, easy preparation, and high luminescence efficiency [12-16]. Lately, a series of new borates with the composition of $MM'_4(BO_3)_3$ (M = Li, Na, K: M' = Ca, Sr, Ba) were synthesized via classic solid-state reaction [17]. The crystal structure and photoluminescence, thermoluminescence and dosimetry properties of novel phosphors ($NaSr_4(BO_3)_3$:Ce^{3+}, $KSr_4(BO_3)_3$:Ce^{3+}) [3, 18]. However, the PL properties of these materials have not been investigated widely. This prompted us to study the fluorescence properties of rare earth ion in the above mentioned borates prepared by combustion synthesis method.

Luminescence materials are usally produced by classical synthesis method (solid state), however, this method have several disadvantages such ashigh reaction temperatures which are energy intensive and thus increase the production costs. This process often results in poor homogenity, additionally size distribution of the powder which affects luminescence efficiency [19]. Combustion method is a novel powder processing technique that can produce ceramic pigments because of a low temperature synthesis technique that offers a unique synthesis route via highly exothermic redox reaction between metal nitrates and an organic fuel to produce ceramic pigments [20]. These processes are characterized by high temperature, fast heating rates and short reaction time. Some other advantages of combustion method are use of relatively simple equipment, formation of high-purity products, stabilization of phases and formation of virtually any size and shape products [21].

By taking the reference of abovestudies on borates in this paper, we foremost reported the photoluminescence and structural properties of $NaCa_4(BO_3)_3$: xEu^{+2}, xCe^{+3} luminescence material prepared via combustion synthesis method.

*Corresponding author:
Tel : +90322 338115
Fax: +903223877115
E-mail: serpil-karakus82@hotmail.com

Experimental

Synthesis of $NaCa_4(BO_3)_3$: xEu^{+2}; xCe^{+3}

Eu^{+2}, Ce^{+3} co-doped $NaCa_4(BO_3)_3$ luminescence material with different molar concentration of europium and cerium (x = 0.03, 0.05, and 0.07) were prepared by the combustion synthesis [20]. High purity starting materials (Aldrich 99%) $NaNO_3$, $Ca(NO_3)_2$, H_3BO_3(as boron source), $CO(NH_2)_2$, $Eu(NO_3)_3$, and $Ce(NO_3)_3$ were used. The stoichiometric amounts of $NaNO_3$,$Ca(NO_3)_2$, H_3BO_3, $CO(NH_2)_2$, $Eu(NO_3)_3$, and $Ce(NO_3)_3$ were dissolved in a minimum amount of distilled water and placed in porcelain containers. The precursor solutions were introduced into muffle furnace and maintained at 550 ºC. The solutions boiled and underwent dehydration, followed by decomposition with the evolution of large amounts gases (N_2, CO_2 etc.) Then, spontaneus ignition occurred and underwent smouldering combustion with enormous swelling, producing white foamy and voluminous ash. The voluminous and foamy combustion ash can be easily milled to obtain the powders [22]. The whole process completed in few minutes. The precursor powders were removed from furnace, and quenched to room tempereture. The well-mixed precursor powders were throughly mixed and then heated up 800 ºC for 2 hrs.

Characterization

The structural analysis of the synthesized materials were examined from XRD patterns using Rigaku RadB-DMAX II diffractometer equipped with Cu K_α (λ = 1.5406 Å) at room temperature. Scanning was generally performed between 10 º and 60 º (2θ) with 0.02 step size. FT-IR (Perkin Elmer Spectrum) were measured at room temperature. The PL excitation and emission spectra were measured with a Shimadzu RF-S301 PC spectrometer equipped with Xe lamp at room temperature. The excitation and emission slits were set to 3.0 nm and 5.0 nm, respectively.The luminescence lifetimes were measured by a laser strobe model TM-3 lifetime fluorophotometer from Photon Technology International (PTI). The morphology was taken with a Brucker SEM and EDX was used.

Results and Discussions

X-ray powder diffraction analysis

The XRD pattern of $NaCa_4(BO_3)_3$ and, Eu^{2+} and Ce^{3+} co-doped $NaCa_4(BO_3)_3$ is presented in Fig. 1, which is agreement with the XRD data of $NaCa_4(BO_3)_3$ reported by Wu et al. [17]. The $NaCa_4(BO_3)_3$ crystallizes in the noncentrosymmetric, orthorhombic structure with space group *Ama2* [17].The foundational building units of $NaCa_4(BO_3)_3$are isolated planar $[BO_3]^{3-}$ groups, which are distributed paralelly along six directions. The Na atoms are eight-coordinated with oxygen atoms to form a distorted bicapped trigonal prism. The Ca atoms

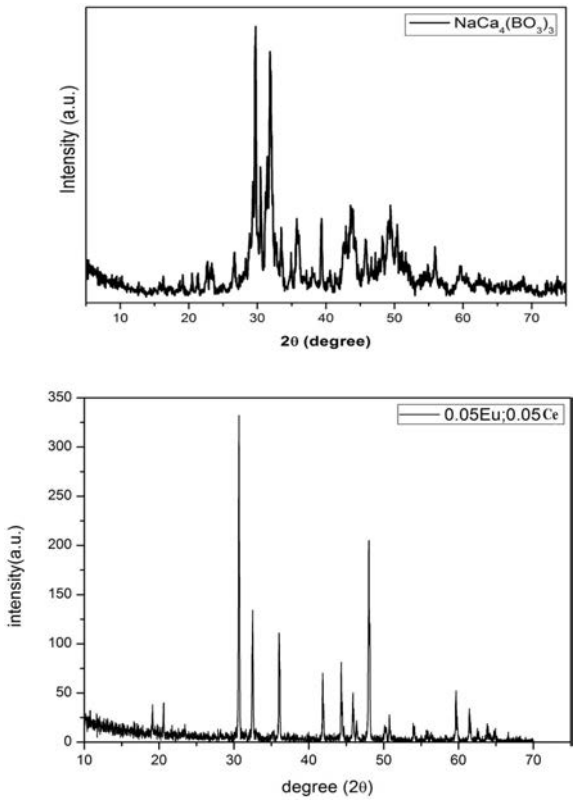

Fig. 1. XRD pattern obtained for $NaCa_4(BO_3)_3$ and $NaCa_{4-2x}(BO_3)_3$:0.05Eu^{2+},0.05Ce^{3+} prepared by acombustion synthesis.

Table 1. The lattice parameters of $NaCa_4(BO_3)_3$:xEu^{2+},xCe^{3+} (x= 0, 0.03, 0.05 and 0.07) luminescence materials calculated from the XRD pattern.

Samples	X	c (Å)	b (Å)	a (Å)	V (Å^3)
$NaCa_4(BO_3)_3$	0	6.48	8.69	10.97	617.82
$NaCa_4(BO_3)_3$: xEu,xCe	0.03	6.63	8.58	10.77	612.66
$NaCa_4(BO_3)_3$: xEu,xCe	0.05	6.54	8.91	11.04	643.22
$NaCa_4(BO_3)_3$: xEu,xCe	0.07	6.54	8.60	10.90	612.57

appear in three crystallographically different environmets [17].

The two possible sites available for incorporation lanthanides in $NaCa_4(BO_3)_3$ lattice are either the Na^+ sites or the Ca^{2+} sites. Because the ionic radius of lanthanide is closer to Ca^{2+} instead of Na^+, it has been considered that the noncentrosymmetric Ca^{2+} sites have been substituted by lanthanide ion in the $NaCa_4(BO_3)_3$ [17]. The lattice parameters of synthesized $NaCa_4(BO_3)_3$:xEu^{2+}, xCe^{3+} were calculated with Pseudo Voight function according to Match 2 program-based Rietvelt structural analysis method. The measured increase in the lattice parameters (*a, b, c,* and *V*) of lanthanide doped $NaCa_4(BO_3)_3$ is an evidence of the displacement between the Ca^+ atoms and lanthanide. Also, the unit cell volume of each lanthanide-doped lattice has increased proportionate

to the amount of lanthanide concentration increasing, especially for x = 0.05, V = 643.22 Å^3, as shown Table 1.

FT-IR spectra of $NaCa_4(BO_3)_3$:xEu^{+2}, xCe^{+3}

To further confirm the coordination environment of B-O in the $NaCa_4(BO_3)_3$structure, the FTIRof $NaCa_4(BO_3)_3$was measured at room temperature. FT-IR revealed prominent absorption with peaks for 1159.73 cm^{-1}, 899.62 cm^{-1}, 735.40 cm^{-1} and 677.99 cm^{-1} (Fig. 2). The IR absorption at wave numbers smaller than 500 cm^{-1} mainly originates from the lattice dynamic modes.The strong bands observed above 1100 cm^{-1} should be assigned to the B-O stretching mode mode of the triangular $[BO_3]^{3-}$ groups, while the bands with the bands with maximum at about 700-900 cm^{-1} may be attributed to the B-O out of plane bending, which confirms the existence of the $[BO_3]^{3-}$ groups. It is found [23]. It is found that there are many closely spaced peaks above 1100 cm^{-1}, which are believed to come from the different bond length of B-O. The absence of peaks in the range of residual nitrate and organic matter. The broad peak at about 3300-3500 cm^{-1} are corresponding to the stretching mode of O-H from the water crystallization in the complex [17, 24, 25].

Morphology of the combustion synthesized $NaCa_4(BO_3)_3$:xEu^{+2}, xCe^{+3}

SEM images are represented in Fig. 3 for combustion synthesized $NaCa_{4-2x}(BO_3)_3$:xEu^{+2}, xCe^{+3} luminescence material. The microstructure of these sample reflects the inherents nature of the combustion process. The particles are highly agglomerated crystallites with foamy and porous surface morphology. The material shows irregular spherical particles, the surface of the foams show alot of cracks, voids and pores. This irregularity in sizes, shapes and porosity may be caused due to the non-uniform distribution of temperature and irregular mass flow during combustion [26]. The EDX spectra confirmed the presence Na, Ca, B, O, Eu, and Ce in Fig. 4.

Photoluminescence of $NaCa_4(BO_3)_3$:xEu^{+2}, xCe^{+3}

Fig. 5 shows the photoluminescence excitation and emission spectrum of $NaCa_{4-2x}(BO_3)_3$:xEu^{+2}, xCe^{+3} (for x = 0.05). Excited by the excitation wavelength of 352 nm, the luminescence material exhibits emission band centered at 445 nm. This is corresponding to the *f-d* transition of Eu^{2+}. The 5*d* energy level of Eu^{2+} and the lower level of 4*f* state overlap, so the electrons of the 4*f*state can be excited to the 5*d* state. The broad luminescence of Eu^{2+} isdue to the $4f^65d^1$-$4f^7$ transition [28].

The luminescence intensities of lanthanide doped phosphors always depend on the doped Eu^{3+}ions concentration [29]. Thus, the photoluminescence spectra of $NaCa_4(BO_3)_3$ with different Eu^{+2}, and Ce^{+3}co-doping concentrations have been indicated Fig. 6. All of the emission spectra exhibit the similar profile with different relative intensities. The emission intesity increases initially with the increase of lanthanide concentration and reaches maximum at x = 0.05, then gradually decreases due to the internal concentration quenching.

According to Blasse, for the critical concentrationthe

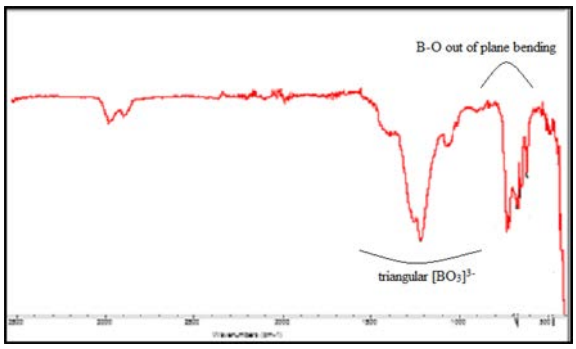

Fig. 2. FT-IR spectra of $NaCa_{4-2x}(BO_3)_3$:xEu^{+2}, xCe^{+3}.

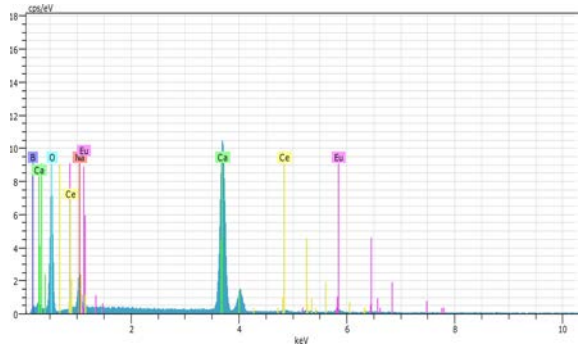

Fig. 4. EDX spectra of $NaCa_{4-2x}(BO_3)_3$:xEu^{+2}, xCe^{+3}.

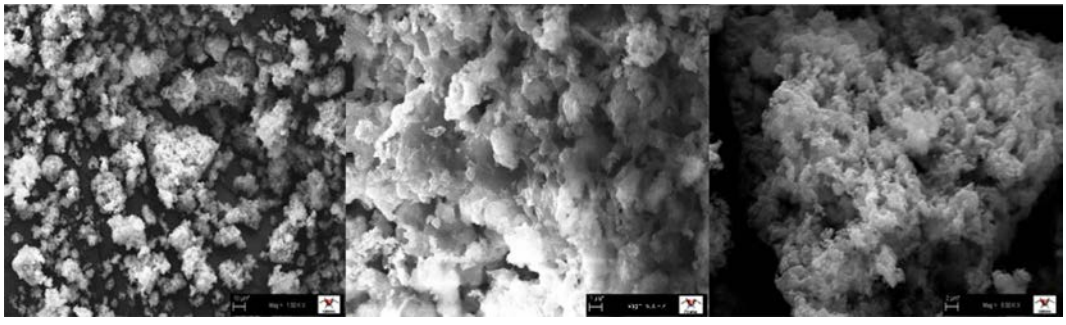

Fig. 3. SEM of combustion synthesized $NaCa_{4-2x}(BO_3)_3$:xEu^{+2},xCe^{+3} under 1 μm to 10 μm.

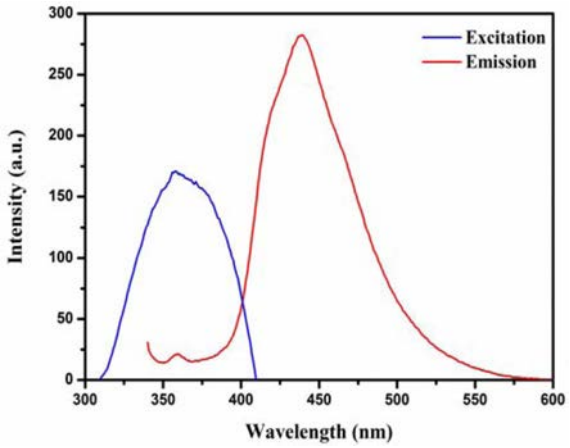

Fig. 5. PL excitation and emission spectra of of $NaCa_{4-2x}(BO_3)_3$:xEu^{+2}, xCe^{+3}.

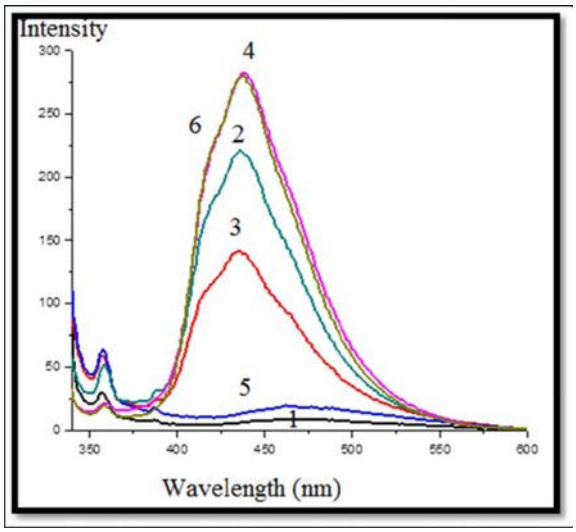

Fig. 6. Comperative excitation (λ_{em}=445 nm) and emission (λ_{ex} = 352 nm) intensity of $NaCa_4(BO_3)_3$: xEu and co-doped $NaCa_{4-2x}(BO_3)_3$: xEu^{+2},xCe^{+3} with different concentrations (x = 0.03, 0.05, 0.07). (1) $NaCa_4(BO_3)_3$:0.03 Eu^{3+}, (2) $NaCa_4(BO_3)_3$:0.03 Eu^{2+}, 0.03Ce^{3+}, (3) $NaCa_4(BO_3)_3$: 0.05 Eu^{3+}, (4) $NaCa_4(BO_3)_3$:0.05 Eu^{2+},0.05Ce^{3+}, (5) $NaCa_4(BO_3)_3$:0.07 Eu^{3+}, and (6) $NaCa_4(BO_3)_3$: 0.07 Eu^{2+},0.07Ce^{3}.

average shortest distance between nearest activator ions is equal to the critical transfer distance R_0. R_0 is, in fact, the critical separation between donor (activator ion) and acceptor (quenching ion), at which the nonradiative rate equals that of the internal single ion relaxation. The R_0 value can be practically calculated using the following equation [29]:

$$R_0 = 2\,(3V/\,4\pi\,x_c\,N)^{1/3} \qquad (1)$$

Where x_c is the critical concentration at which quenching occurs, N the number of Ca^{2+} ions in the $NaCa_4(BO_3)_3$unit cell, and V the volume of the unit cell. By taking experimental and analytic data of x_c, N, and V, the critical transfer distance of was determinated to be 26 Å. The luminescence lifetimes in $NaCa_4(BO_3)_3$:xEu^{2+}, xCe^{3+} with different concentrations were measured, and they are shown in Fig. 7. The derived lifetime from the decay curve is about 1.15 ns (for x = 0.05).

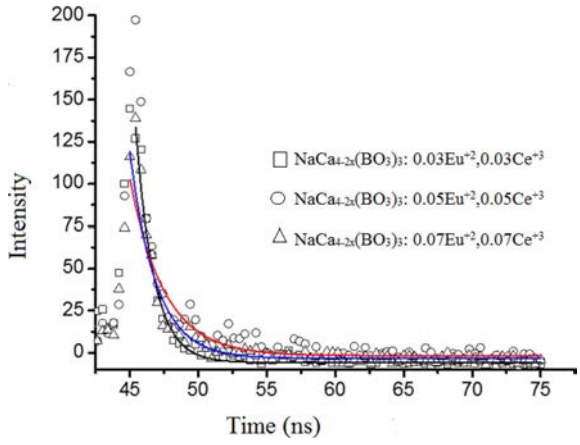

Fig 7. Decay curve of $NaCa_4(BO_3)_3$:xEu^{2+}, xCe^{3+}.

Conclusions

Eu^{+2} and Ce^{+3} co-doped $NaCa_4(BO_3)_3$ luminescence materials were prepared by combustion synthesis method followed by heatingof the precursor combustion ash at 800 ºC in air for 2 hrs. The XRD pattern of $NaCa_4(BO_3)_3$ prepared by the combustion method is in good agreement with the XRD data of $NaCa_4(BO_3)_3$ reported by Wu et al. The synthesized materials show intense emission at 445 nm. The PL spectrum at verious doping concentration of lanthanides shows maximum emission at x = 0.05 after the concentration quenching is observed and, the calculated critical distance of concentration quenching is 26 Å. The fitted fluorescence lifetime is 1.15 ns for x = 0.05. This fundamental work might be important for the fields of lamps and display due to the decay time of the luminescence is enough short. In addition, The combustion synthesis technique is faster and cheaper other synthesis methods such as solid-state and, sol-gel processes.

Acknowledgments

The authors are also thankful the National Boron Research Institute (BOREN) for financial support to this work with the project no: 2013.Ç0410.

References

1. X. Chen, C. Yang, X. Chang, H. Zang, W. Xiao, J. Alloys Compd. 492 (2010) 543.
2. P. Li, L. Pang, Z. Wang, Z. Yang, Q. Guo, X. Li, J. Alloys Compd. 478 (2009) 813.
3. L.H. Jiangh, Y.L. Zhang, C.Y. Li, J.Q. Hao, Q.J. Su, J. Alloys Compd. 82 (2009) 313.

4. Y. Huang, W. Zhao, L. Shi, H.J. Seo, J. Alloys Compd. 477 (2009) 936.
5. E.J. Popovici, M. Nazarov, L. Muresan, D.Y. Noh, L.B. Tudoran, E. Bica, E. Indrea, J. Alloys Compd. 497 (2010) 201.
6. A. Majchrowski, S. Klosowicz, L.R. Jaroszewicz, M. Swirkowicz, I.V. Kityk, M. Piasecki, M.G. Brik, J. Alloys Compd. 491 (2010) 26.
7. X. Zhang, H.J. Seo, J. Alloys Compd. 503 (2010) L14-L17.
8. S. Shionoya, W.M. Yen, Phosphor Handbook, CRC Press, 1999.
9. X.M. Zhang, X. Qiao, H.J. Seo, J. Electrochem. Soc. 157 (2010) J267.
10. G. Li, Y. Lai, T. Cui, H. Yu, D. Liu, S. Gan, Mater. Chem. Phys. 124 (2010) 1094.
11. H.Y. Jiao, Y.H. Wang, Appl. Phys. B: Lasers Opt. 98 (2010) 423.
12. X. Zhang X, H.J. Seo H J, Physica B 406 (2011) 77-79.
13. D. Yashashchandra, R.S. Bahadur, J. Am. Ceram. Soc. 93 (2010) 56.
14. H. Zhang, Y. Wang, Y. Tao, W. Li, D. Hu, E. Feng, X. Nie, J. Electrochem. Soc. 157 (2010) J293.
15. Y. Yang, L. Yu, C. Tao, Z. Dai, H. Yang, J. Electrochem. Soc. 25 (2010) 56.
16. M.A.K. Elfayoumi, M. Farouk, M.G. Brik, M.M. Elokr, J. Alloys Compd. 492 (2010) 712.
17. L. Wu, X.L. Chen, Y.P. Xu, Y.P. Sun, Inorg. Chem. 45 (2006) 3042.
18. Jiang L, Zhang Y, Li C, Pang R, Shi L, Zhang S, Hao J, Su Q, J. Rare Earths, 2009, 27, 429.
19. Y.Z. Halefoğlu, E. Kusvuran, Journal Ceramic Processing Recearch 11[1] (2010) 92- 95.
20. Y.Z. Halefoglu, O. Serindag, Journal of Ceramic Processing Research 15[4] (2014) 262-265.
21. K.C. Patil, S.T. Aruna, T. Mimani, Solid-State and Material Science 6 (2002) 507-512
22. C. Zhao, D. Chen, Materials Letters 61 (2007) 3673-3675.
23. C.F. Guo, Q. Tang, C.X. Zhang, D.X. Huang, Q. Su, J. Lumin. 126 (2007) 333-337.
24. A. Rulmont, M. Almou, Spectrochim. Acta A45 (1989) 603-608.
25. P.K. Sharma, R. Nass, H. Schmidt, Opt. Mater. 10 (1998) 161-169.
26. N.S. Bajaj, S.K. Omanwar, Optical Materials 35 (2013) 1222-1225.
27. A.B. Gawande, R.P. Sonekar, S.K. Omavwar, International Journal of Optics, Article ID 418459 (2014) 6.
28. S.S. Yao, L,H. Xue, Y.W. Yan, Current Applied Physics 11 (2011) 639-642.
29. A.B. Gawande, R.P. Sonekar, S.K. Omavwar, Journal of Luminescence 149 (2014) 200-203.